Modeling the doubly excited state with time-dependent Hartree–Fock and density functional theories

Christine M. Isborn and Xiaosong Li

Citation: The Journal of Chemical Physics **129**, 204107 (2008); doi: 10.1063/1.3020336
View online: http://dx.doi.org/10.1063/1.3020336
View Table of Contents: http://aip.scitation.org/toc/jcp/129/20
Published by the American Institute of Physics

Modeling the doubly excited state with time-dependent Hartree–Fock and density functional theories

Christine M. Isborn and Xiaosong Li[a)]
Department of Chemistry, University of Washington, Seattle, Washington 98195-1700, USA

(Received 2 July 2008; accepted 15 October 2008; published online 25 November 2008)

Multielectron excited states have become a hot topic in many cutting-edge research fields, such as the photophysics of polyenes and in the possibility of multiexciton generation in quantum dots for the purpose of increasing solar cell efficiency. However, obtaining multielectron excited states has been a major obstacle as it is often done with multiconfigurational methods, which involve formidable computational cost for large systems. Although they are computationally much cheaper than multiconfigurational wave function based methods, linear response adiabatic time-dependent Hartree–Fock (TDHF) and density functional theory (TDDFT) are generally considered incapable of obtaining multielectron excited states. We have developed a real-time TDHF and adiabatic TDDFT approach that is beyond the perturbative regime. We show that TDHF/TDDFT is able to simultaneously excite two electrons from the ground state to the doubly excited state and that the real-time TDHF/TDDFT implicitly includes double excitation within a superposition state. We also present a multireference linear response theory to show that the real-time electron density response corresponds to a superposition of perturbative linear responses of the S_0 and S_2 states. As a result, the energy of the two-electron doubly excited state can be obtained with several different approaches. This is done within the adiabatic approximation of TDDFT, a realm in which the doubly excited state has been deemed missing. We report results on simple two-electron systems, including the energies and dipole moments for the two-electron excited states of H_2 and HeH^+. These results are compared to those obtained with the full configuration interaction method. © *2008 American Institute of Physics*. [DOI: 10.1063/1.3020336]

I. INTRODUCTION

With new insights addressed in experimental sciences and technologies, such as molecular optical response in high-intensity fields, electron transductivity in molecular devices, and effectiveness of solar energy conversion, there is an increasing demand for modeling molecular excited states.[1,2] Particularly, multielectron excited states have been found to be especially important in the photophysics of polyenes since the low-lying A_g state has significant double-excitation character.[3–6] In addition, the possibility of multiexciton generation in quantum dots[7–9] has also led to increased interest in modeling multielectron excited states because understanding this process could be the key to enhancing solar cell efficiency. However, calculating multielectron excited states has been a major obstacle as it is often done with multiconfigurational methods, such as complete active space self-consistent field (CASSCF) or symmetry-adapted cluster-configuration interaction (SAC-CI) methods, which incur formidable computational cost for large systems.

For a single-configuration based approach, excitations are either approximated with single-electron transitions between molecular orbitals (MOs) or obtained by time-dependent Hartree–Fock[10,11] (TDHF) and density functional theory (TDDFT).[12–14] TDHF and TDDFT are single Slater determinant approximations to the full expansion of the time-dependent Schrödinger equation over all the excited states. TDHF and TDDFT avoid the explicit calculation of excited state wave functions by instead following the dynamics of a superposition state. Because TDHF/TDDFT is a single-configuration methodology, it is quite affordable and has promise for modeling electron dynamics of fairly large systems. TDDFT[12,13] within the Kohn–Sham (KS) framework is implemented similarly to TDHF, but in principle, includes all many-body correlation effects through the exact frequency-dependent exchange-correlation kernel. In practice the kernel is generally approximated with a time-independent adiabatic exchange-correlation functional. Within this adiabatic approximation, the exchange-correlation potential is determined only by the instantaneous electron density.

There are two common implementations of TDHF/TDDFT: linear response and real-time propagation. The former implementation is the most common; the TDHF/TDDFT equations are linearized, keeping only the first order (linear) response to an applied perturbation.[11,15–19] Within the realm of nuclear physics, the linear response TDHF method is known as the random phase approximation.[20–22] This method is generally performed in the frequency domain and for the most part uses the HF/DFT ground state as a reference. The linear response equation in matrix form is

[a)]Author to whom correspondence should be addressed. Electronic mail: li@chem.washington.edu.

$$\begin{bmatrix} \mathbf{A} & \mathbf{B} \\ \mathbf{B}^* & \mathbf{A}^* \end{bmatrix} \begin{bmatrix} \mathbf{X} \\ \mathbf{Y} \end{bmatrix} = \omega \begin{bmatrix} 1 & 0 \\ 0 & -1 \end{bmatrix} \begin{bmatrix} \mathbf{X} \\ \mathbf{Y} \end{bmatrix},$$

$$A_{ia,jb} = (\varepsilon_a - \varepsilon_i)\delta_{ij}\delta_{ab} + (ia\|jb), \tag{1}$$

$$B_{ia,jb} = (ia\|bj), \tag{2}$$

where **X** and **Y** are the electron density responses determined by solving this linear equation, ε is the orbital energy, $(ia\|jb)$ is the antisymmetrized two-electron integral, which includes both Coulomb and exchange (and correlation in TDDFT) terms, and ω is a matrix of eigenvalues representing the transition energies of the system. We here use the common notation, in which i,j represent occupied orbitals, and a,b are virtual orbitals of the ground state configuration. Because it is superior in accuracy to MO energy differences and computationally much cheaper than multiconfigurational wave function based methods, linear response adiabatic TDHF/TDDFT has become the tool of choice for calculating the photophysical properties of molecules.

The second implementation is propagating the TDHF/TDDFT equations in real time, fully taking into account the change in the electron-electron potential as a result of the changing density.[10,13,23–25] Because this method includes the full response of all electrons, it nonperturbatively models nonadiabatic multielectron dynamics and is thus suitable for modeling molecular interactions with intense fields. Real-time TDHF/TDDFT simulations agree with linear response TDHF/TDDFT in the weak field off-resonance limit,[29] but also include the nonlinear response to all orders and can be use to calculate nonlinear response properties.[13,26–28] Real-time TDHF/TDDFT has already been used to simulate strong laser fields interacting with linear polyenes, polyacenes, and their cations,[30–32] but the applied field frequency ω has remained off-resonance with molecular excitation, thus not significantly altering the ground state electron density.

Going beyond the linear response[33–35] allows treatment of nonlinear properties, such as the calculation of frequency-dependent hyperpolarizabilities[34–36] and the simultaneous absorption of multiple photons, as in two-photon absorption.[37–39] However, one of the major downfalls of adiabatic TDHF/TDDFT is that it is generally considered incapable of obtaining multiple-electron excited states.[6,11,15,16,40–44] Tretiak and Chernyak showed that doubly excited states can be calculated within adiabatic TDDFT by going beyond the linear response regime.[33] The transition energies of the quadratic response doubly excited states, however, appear at excitation energies that are simply the sum of the linear response excitation energies. Work by Maitra and co-workers[40,45] shows that it is necessary to go beyond the adiabatic approximation of TDDFT with the use of a nonadiabatic frequency-dependent kernel in order to obtain the correct excitation energies of doubly excited states.

In this work we present molecular two-electron excited states obtained with real-time TDHF and the adiabatic approximation of TDDFT. Two-electron–two-orbital H_2 and HeH^+ systems are used for simplicity. Although we plan to address the effects of a spin-dependent field in a future publication, this work follows the standard implementation of a spin-independent perturbation within real-time TDHF/TDDFT, i.e., an applied field that excites both α and β electrons simultaneously. We maintain a closed-shell system as we resonantly excite both electrons from the ground state to the doubly excited state. We show distinctions and connections between the way the doubly excited state can be represented in the linear response and real-time propagation methods.

II. THEORY

A. Real-time TDHF/TDDFT

We use the method described in Refs. 23 and 46–48, in which we explicitly evolve the electron density in the time domain. In our implementation of TDHF/TDDFT, the two-electron potential in the Hamiltonian is time dependent during the time evolution of the electronic degrees of freedom. Real-time TDHF and TDDFT methods allow nonadiabatic perturbative treatment of electron dynamics by updating the two-electron potential in the Hamiltonian with the evolving electron distribution. With the electronic wave function represented by a single Slater determinant of single particle MOs φ_i, the time-dependent Schrödinger equation [a.u. $(e=m_e=\hbar=1)$ is used throughout] reduces to the TDHF equation or the time-dependent KS equation,

$$i\frac{\partial \varphi_i(t)}{\partial t} = \hat{H}(t)\varphi_i(t), \tag{3}$$

the MOs are represented as a linear combination of atomic orbital (AO) basis functions χ_μ as

$$\varphi_i(t) = \sum_\mu c_{\mu,i}(t)\chi_\mu, \tag{4}$$

where we allow the time-dependent coefficients to be complex. The full time-dependent Hamiltonian $\hat{H}$ includes both the external potential field and the field-free Hamiltonian $\hat{H}_0$, which represents the molecular internal potential that electrons experience at a given time,

$$\hat{H}_0(t) = \hat{h}(t) + \hat{G}(t). \tag{5}$$

The one-electron operator $\hat{h}(t)$ includes the electron kinetic energy operator and the electron-nuclear attractive potential,

$$\hat{h}(t) = -\sum_{i=1}^{N_e} \frac{1}{2}\Delta_i^2 - \sum_{i=1}^{N_e}\sum_{\alpha=1}^{N_n} \frac{Z_\alpha}{|\mathbf{r}_i - \mathbf{R}_\alpha|}. \tag{6}$$

When the nuclei are fixed, the one-electron operator becomes time independent $\hat{h}(t)=\hat{h}(t=0)$. The two-electron operator $\hat{G}(\rho(t))$ introduces the electron-electron interactive potential. $\hat{G}(\rho(t))$ is inherently time dependent because it depends on the instantaneous electron distribution at a given time. In the adiabatic KS-DFT formalism, $\hat{G}(\rho(t))$ includes the Coulomb (also called Hartree) and exchange-correlation potentials

$$\hat{G}(t) = \int \frac{\rho(\mathbf{r}',t)}{|\mathbf{r}-\mathbf{r}'|} d\mathbf{r}' + V_{\mathrm{xc}}[\rho](\mathbf{r},t)$$
$$\approx \int \frac{\rho(\mathbf{r}',t)}{|\mathbf{r}-\mathbf{r}'|} d\mathbf{r}' + V_{\mathrm{xc}}[\rho_t](\mathbf{r}). \quad (7)$$

In the above notation we are explicitly indicating the adiabatic approximation within DFT, in which the exchange-correlation potential V_{xc} has no "memory" of previous time steps and only depends on the instantaneous time-dependent density $\rho(\mathbf{r},t)$ at a particular time: $V_{\mathrm{xc}}[\rho](\mathbf{r},t) \approx V_{\mathrm{xc}}[\rho_t](\mathbf{r})$.

We use an orthonormal basis by transforming the density and Fock/KS matrices from the AO basis via a Löwdin transformation (for transformation from AO to orthonormal basis, see Refs. 23, 47, and 48). In an orthonormal basis, the TDHF/TDDFT equations can be represented in matrix form as

$$i\frac{\mathbf{P}(t)}{\partial t} = [\mathbf{H}(t), \mathbf{P}(t)], \quad (8)$$

where $\mathbf{P}$ and $\mathbf{H}$ are density and Fock/KS matrices with matrix elements $P_{\mu\nu} = \Sigma_i c^{\dagger}_{\mu,i} c_{\nu,i}$ and $H_{\mu\nu} = \langle \chi_\mu | \hat{H} | \chi_\nu \rangle$. The time dependence of the Hamiltonian includes perturbation from the external field but also depends on the time dependence of the instantaneous two-electron potential arising from time-dependent electron distribution.

Within real-time methods, propagation of electronic degrees of freedom using a time-dependent Hamiltonian, perturbative or nonperturbative, can be done using various algorithms, such as split operator and unitary transformation methods. In this paper, we propagate the electron density in real time with a midpoint unitary transformation containing the eigenvectors $\mathbf{C}$ and eigenvalues ε of the time-dependent Fock/KS matrix at time t_k,

$$\mathbf{P}(t_{k+1}) = \mathbf{U}(t_k)\mathbf{P}(t_{k-1})\mathbf{U}^{\dagger}(t_k), \quad (9)$$

$$\mathbf{U}(t_k) = \exp(i\mathbf{H}(t_k)2\Delta t) = \mathbf{C}(t_k)\exp(i\varepsilon(t_k)2\Delta t)\mathbf{C}^{\dagger}(t_k). \quad (10)$$

This method takes into account linear changes in both the density and external field during the short time step while maintainting the idempotency of the density matrix ($\mathbf{P} = \mathbf{P}\cdot\mathbf{P}$).

The instantaneous electron occupation N_i of an MO can be analyzed by projection onto the undressed eigenspace $\mathbf{C}(t=0)$,

$$N_i(t) = \mathbf{C}_i^{\dagger}(0)\mathbf{P}(t)\mathbf{C}_i(0), \quad (11)$$

where $\mathbf{C}_i(0)$ is the ith eigenvector of the field-free Fock/KS matrix. In our simulations, we use a linearly polarized and spatially homogeneous external field (the dipole approximation) of frequency ω, in the length gauge,

$$V_{\mathrm{ext}} = \mathbf{E}(\mathbf{r},t)\cdot\mathbf{d} \approx \mathbf{E}(0,t)\cdot\mathbf{d} = \mathbf{E}_{\max}\cdot\mathbf{d}\,\sin(\omega t), \quad (12)$$

where $\mathbf{d}$ is the electric dipole integral $d_{\mu\nu} = \langle \chi_\mu | \hat{r} | \chi_\nu \rangle$.

B. Linear response of a superposition state: A multireference linear response theory

In this work, simple two-electron–two-orbital systems, H_2 and HeH^+, are used for the sake of a clear presentation of theory and observation, and we restrict our linear response analysis to these systems. A two-electron–two-orbital ($\varphi_1 = \sigma$ and $\varphi_2 = \sigma^*$) system has six possible configurations (Slater determinants): $|\sigma(\alpha)\sigma(\beta)\rangle$, $|\sigma(\alpha)\sigma^*(\beta)\rangle$, $|\sigma(\beta)\sigma^*(\alpha)\rangle$,$|\sigma(\alpha)\sigma^*(\alpha)\rangle$, $|\sigma(\beta)\sigma^*(\beta)\rangle$, and $|\sigma^*(\alpha)\sigma^*(\beta)\rangle$. These configurations give rise to three singlet states (many-electron wave functions) within the configuration interaction (CI) scheme: S_0 is dominated by the $|\sigma(\alpha)\sigma(\beta)\rangle$ configuration having two electrons in the bonding σ orbital, with some admixture of the doubly excited configuration $|\sigma^*(\alpha)\sigma^*(\beta)\rangle$, which puts both electrons in the antibonding σ^* orbital; the first excited singlet state S_1 is a symmetry adapted combination of the two open-shell configurations, $|\sigma(\alpha)\sigma^*(\beta)\rangle$ and $|\sigma(\beta)\sigma^*(\alpha)\rangle$; the second excited singlet state S_2 is dominated by the doubly excited $|\sigma^*(\alpha)\sigma^*(\beta)\rangle$ configuration having two electrons in the antibonding orbital, with some admixture of the $|\sigma(\alpha)\sigma(\beta)\rangle$ configuration. For simplification, we denote the $|\sigma(\alpha)\sigma(\beta)\rangle$ configuration as ψ_{S_0} and the the doubly excited $|\sigma^*(\alpha)\sigma^*(\beta)\rangle$ configuration as ψ_{S_2}.

Using the real-time TDHF/TDDFT method presented in Sec. II A, we use a resonant field to drive both the α and β electrons from the S_0 state to the S_2 state. Within a closed-shell description of the electron time evolution, the single-configuration wave function does not contain the open-shell configurations. The superposition state of our real-time TDHF/TDDFT wave function can then be expanded in configuration space as

$$\Psi = C_{S_0}\psi_{S_0} + C_{S_2}\psi_{S_2}, \quad (13)$$

where the expansion coefficients C are time dependent. The total density matrix of this superposition state is

$$\mathbf{P}^{(0)} = C^2_{S_0}\mathbf{P}_{S_0} + C^2_{S_2}\mathbf{P}_{S_2}. \quad (14)$$

The density matrix form of the TDHF/TDDFT equation [Eq. (8)] is often used as a starting point in deriving the linear response equations of TDHF/TDDFT. The electron density matrix is expanded to first order in the perturbation,

$$\mathbf{P} = \mathbf{P}^{(0)} + \mathbf{P}^{(1)}, \quad (15)$$

and the HF/KS first order response $\mathbf{H}^{(1)}$ is formed as a sum of the applied perturbation and first order response of the electron-electron interaction $\mathbf{G}(\mathbf{P}^{(1)})$. The first order response of the density matrix can be written as

$$\mathbf{P}^{(1)} = \delta\mathbf{P}e^{-i\bar{\omega}t} + \delta\mathbf{P}^* e^{i\bar{\omega}t}, \quad (16)$$

$$\delta P_{ia} e^{-i\bar{\omega}t} = (C^2_{S_0}\delta P_{S_0,ia} - C^2_{S_2}\delta P_{S_2,ia})e^{-i\bar{\omega}t}, \quad (17)$$

$$\delta P^*_{ai} e^{i\bar{\omega}t} = (C^2_{S_0}\delta P_{S_0,ai} - C^2_{S_2}\delta P_{S_2,ai})e^{i\bar{\omega}t}. \quad (18)$$

Equations (17) and (18) indicate that the density response oscillates at a collective frequency $\bar{\omega}$ that represents a superposition of transitions from the participating configurations of the reference state. Following the regular TDHF/TDDFT

derivations, Eqs. (17) and (18) give rise to a non-Hermitian eigenvalue problem similar to that commonly used in response theory

$$\begin{bmatrix} \mathbf{A} & \mathbf{B} \\ \mathbf{B}^* & \mathbf{A}^* \end{bmatrix} \begin{bmatrix} \mathbf{X} \\ \mathbf{Y} \end{bmatrix} = \bar{\omega} \begin{bmatrix} 1 & 0 \\ 0 & -1 \end{bmatrix} \begin{bmatrix} \mathbf{X} \\ \mathbf{Y} \end{bmatrix},$$

$$A_{ia,jb} = [C_{S_0}^2(\varepsilon_{S_0,a} - \varepsilon_{S_0,i}) - C_{S_2}^2(\varepsilon_{S_2,a} - \varepsilon_{S_2,i})]\delta_{ij}\delta_{ab} + C_{S_0}^2(ia\|jb)_{S_0} - C_{S_2}^2(ia\|jb)_{S_2}, \quad (19)$$

$$B_{ia,jb} = C_{S_0}^2(ia\|bj)_{S_0} - C_{S_2}^2(ia\|bj)_{S_2}, \quad (20)$$

where the perturbation densities are $X_{ia} = \delta P_{ia}$ and $Y_{ia} = \delta P_{ai}$. Here i,j and a,b represent occupied and virtual MOs, respectively, of the subscripted configuration. Note that two-electron integrals, MOs, and their energies are dependent on the electron configuration.

The solution of the linear response function for a superposition state is a function of the expansion coefficients C in Eq. (13). Thus, as the superposition state propagates away from the ground state, the observed density response changes. If $C_{S_0} = 1$, the solution is the usual linear response of the ground state configuration, giving rise to the one-electron $S_0 \rightarrow S_1$ transition energy. For our two-electron system with the ground state as the reference, the σ orbital is doubly occupied and the diagonals of the **A** matrix include the difference in energy between the occupied σ orbital and the virtual σ^* orbital. If, however, $C_{S_2} = 1$, the doubly excited configuration is the reference for the linear response. For this reference configuration, the σ orbital is unoccupied and σ^* is doubly occupied. The diagonals of the **A** matrix then include the difference in energy between the occupied σ^* orbital and the unoccupied σ orbital. The energy obtained using the doubly excited configuration as the reference is then the de-excitation energy to the singly excited state, $S_2 \rightarrow S_1$, in the linear response framework. Therefore, as a result of the perturbation to the superposition state wave function consisting of both ground and doubly excited configurations, the real-time propagation method is equivalent to an average of excitation from the ground state and de-excitation from the doubly excited state.

III. RESULTS AND DISCUSSION

We use the development version of the GAUSSIAN code[49] with the STO-3G basis set to obtain the initial wave function and to calculate the one- and two-electron integrals for the Hamiltonian that is a function of the evolving density. Three different time-dependent Hamiltonians are implemented: HF, the adiabatic local spin density approximation (LSDA),[50] and the generalized gradient approximation of Perdew–Burke–Ernzerhof (PBE).[51] The simulations begin with the molecule initially in its field-free ground state as determined by the corresponding time-independent methods. The bond length of H_2 is fixed at 0.7331 Å and that for HeH^+ at 0.9295 Å, with the two atoms equally spaced from the origin. For simplicity we ignore all nuclear motion. However, with intense fields causing excitation, the bond length of H_2 would increase, and in the S_2 state the molecule would no longer be bound within this minimal basis.

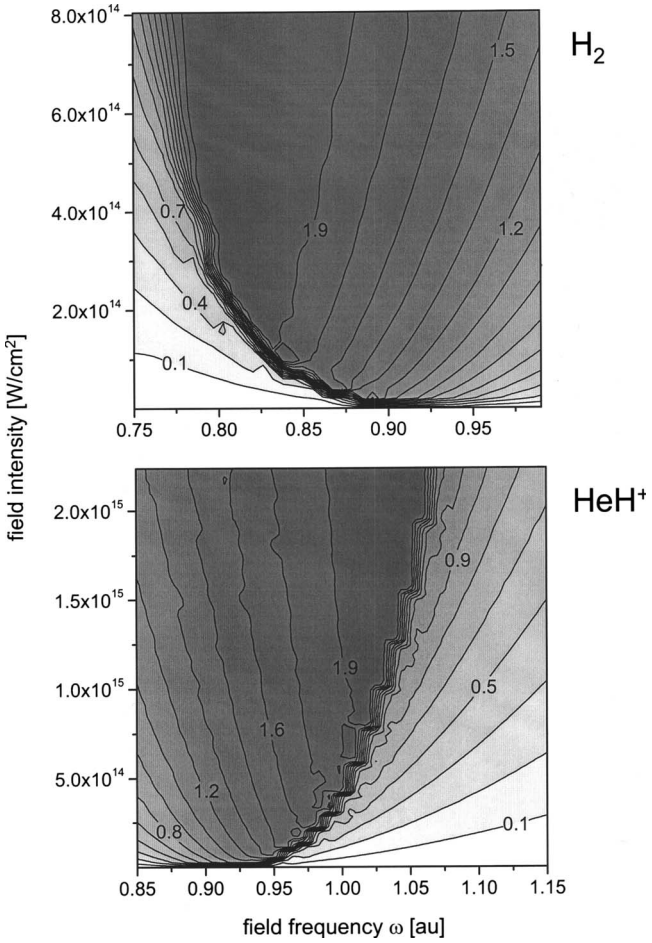

FIG. 1. TDHF maximum population of the antibonding σ^* orbital for H_2 and HeH^+ as a function of applied field intensity (W/cm^2) and field frequency (a.u.).

The initial state is propagated in real time using the method described in Sec. II A. The electric field vector is applied along the molecular axis for varying amounts of time, and we use an integration time step of 0.002 fs in propagating the wave function. During propagation, the time-dependent wave function is projected onto the initial state, giving the occupation of the time-independent starting orbitals.

For H_2 and HeH^+, using a minimal basis multiconfigurational method that accounts for the doubly excited state within the electric dipole approximation and assuming non-degenerate transtions, there are two peaks in the absorption spectrum: one for $S_0 \rightarrow S_1$ and another for $S_1 \rightarrow S_2$. Within the standard ground state implementation of linear response adiabatic TDHF/TDDFT, only the $S_0 \rightarrow S_1$ transition exists. One would thus expect the resonant field frequency for population inversion to occur at the single-electron transition energy given by linear response theory TDHF/TDDFT. Since nonlinear response calculations[33] have found the energy of the doubly excited state to simply correspond to the sum of the singly excited state energies, one would also expect the excitation energy of the doubly excited state in these two-electron–two-orbital systems to be twice the excitation en-

TABLE I. For minimal basis H_2 and HeH^+, energy gaps (in a.u.) between the ground S_0 and doubly excited S_2 states, and the linear response (LR) singly excited $S_0 \rightarrow S_1$ excitation energies. The singly-excited state energy gap is calculated with perturbative linear response (LR) methods, and the $S_0 \rightarrow S_2$ energy gap is calculated with the nonperturbative real-time TDHF and TDDFT approaches. The relevant full CI results are also shown for comparison.

Method	$\Delta E_{S_0 \rightarrow S_2}$	$\mathrm{LR}\Delta E_{S_0 \rightarrow S_1}$
	H_2	
HF	1.596	0.939
LSDA	1.519	0.953
PBE	1.492	0.946
CI	1.637	0.977[a]
	HeH^+	
HF	2.153	0.902
LSDA	2.135	0.864
PBE	2.140	0.854
CI	2.166	0.834[a]

[a]The full CI results are not calculated within the LR formalism.

ergy of the linear response TDHF/TDDFT singly excited state. However, this is not the case in real-time TDHF/TDDFT simulations. By tuning the field frequency ω and the field intensity within our real-time adiabatic TDHF/TDDFT simulations, we can drive both electrons of H_2 and HeH^+ from the ground state bonding σ orbital into the antibonding σ^* orbital. Beginning with H_2 and HeH^+ in a converged ground state, we swept through a number of field intensities and frequencies. Figure 1 shows contour plots for the TDHF field-on electron optical response from the ground state. Full population inversion occurs at external field frequencies $\omega \approx 0.80$ and ≈ 1.05 a.u. for H_2 and HeH^+, respectively. This resonant field frequency is certainly not expected from the linear response framework of the TDHF theory, which predicts $S_0 \rightarrow S_1$ excitation energies at 0.94 and 0.90 a.u. (see Table I).

The reason for the difference between the real-time propagation resonant field frequencies and the linear response theory excitation energies lies in the treatment of the two-electron potential. In common response theory, the ground state electron distribution is used to obtain the one-electron excitations. In real-time TDHF/TDDFT, the potential is a linear combination of the ground and doubly excited state potentials. The average potential an electron sees will differ from the ground state potential due to the excitation of other electrons. As a result, for H_2 and HeH^+, our TDHF resonant field frequency represents an average solution of the response function: that for the potential of the ground state S_0 and that for the potential of the doubly excited state S_2. As shown in Sec. II, the electron density response in real-time TDHF/TDDFT is a superposition of $S_0 \rightarrow S_1$ and $S_2 \rightarrow S_1$. We will discuss two important consequences of this superposition response: (1) resonant behavior does not occur at the $S_0 \rightarrow S_1$ energy gap, and (2) the doubly excited state is implicitly included in the propagation, and its energy can be obtained by direct computation using the electron density of the excited state (Sec. III A) or by analyzing the oscillation of the residual dipole (Sec. III C). In this article we present discussions mainly for the TDHF results for clarity, but a similar phenomenon is observed for the TDDFT electron dynamics.

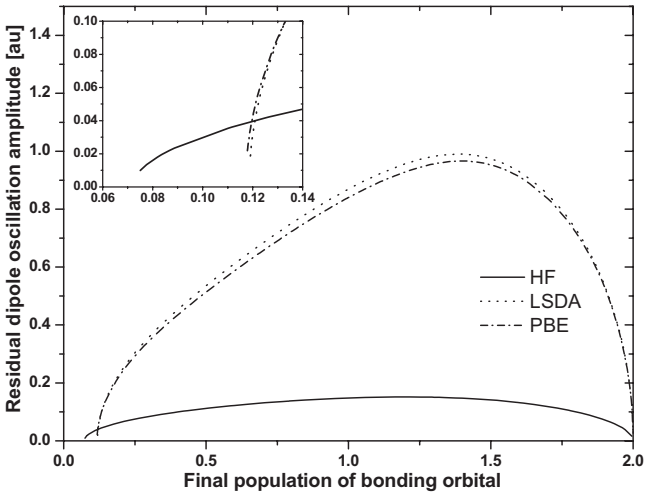

FIG. 2. Residual dipole oscillation amplitude for HeH^+ as a function of excitation from the ground state.

A. Energy of the doubly excited S_2 state

In a stationary state, the density matrix commutes with the Fock matrix, and neither the density nor the dipole oscillates. We determine the density of the S_2 state of H_2 and HeH^+ as the point of least oscillation. For H_2, this occurs when the ground state antibonding σ^* orbital is doubly occupied. For HeH^+, the point of smallest dipole oscillation amplitude occurs when the ground state antibonding σ^* orbital is mostly occupied. Figure 2 shows the HeH^+ dipole oscillation amplitude as a function of population of the bonding orbital. While it is clear that the TDDFT dipole response is much larger than the TDHF response, which will be discussed in a future publication, we focus on the point where the dipole oscillation amplitude goes to zero. For the TDHF simulations, this occurs at a σ population of $0.07e$ and for TDLSDA and TDPBE simulations at $0.12e$. We thus take this occupation to be that of the S_2 state. Even without the presence of a perturbing field, starting the HeH^+ simulations with the σ^* orbital doubly occupied leads to population oscillation, indicating that a complete double occupation of σ^* is not a stationary state of the Fock/KS Hamiltonian for HeH^+.

In this section we show the distinction between the energy of the doubly excited state as calculated by traditional response theory (which predicts a value of $2 \times \Delta E_{S_0 \rightarrow S_1}$) and that calculated from the electron density by HF/DFT after using real-time TDHF/TDDFT to resonantly drive the electron density into the S_2 state. The HF energy can be computed directly from this electron density distribution, $E = \mathrm{Tr}[(\mathbf{h} + 1/2\mathbf{G}(\mathbf{P}))\mathbf{P}]$. The DFT energy includes exchange and correlation contributions as calculated by the adiabatic exchange-correlation functional $V_{xc}[\rho]$. Table I lists HF and DFT $S_0 \rightarrow S_2$ energy gaps. For comparison, we also include the full CI results.

In comparison to the fully correlated CI results, the HF

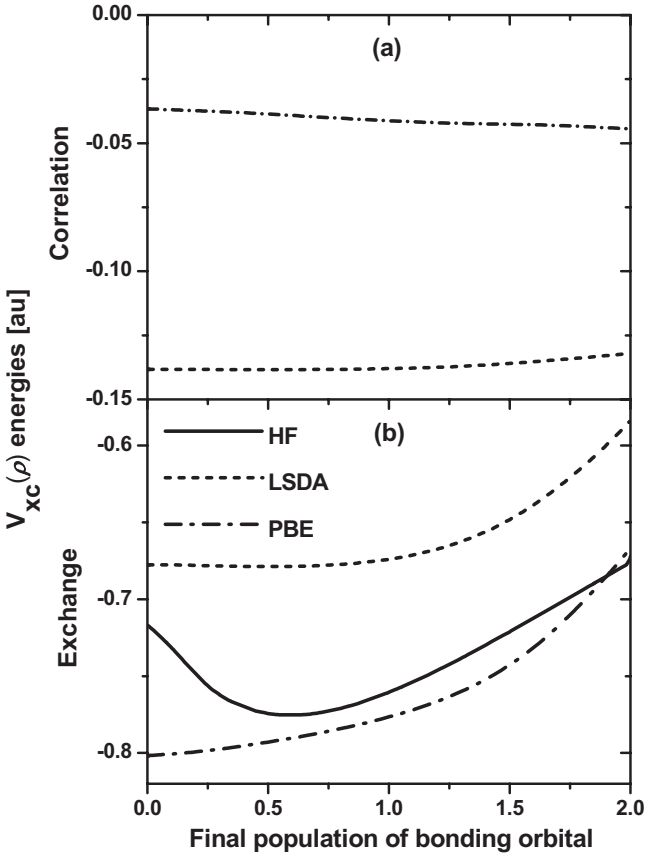

FIG. 3. DFT (a) correlation and (b) exchange energies for H_2 as a function of excitation from the ground state.

ground state for H_2 is ~0.02 a.u. higher, and the doubly excited state is ~0.02 a.u. lower in energy, leading to a smaller energy gap between the two states. The LSDA and PBE functionals are used to calculate the energies of the S_0 and S_2 states, knowing from the outset that the adiabatic KS exchange-correlation functional is designed to reproduce ground state interacting densities, rather than excited state interacting densities. The LSDA and PBE energy gaps (Table I) for $S_0 \rightarrow S_2$ are smaller than that calculated with HF. The DFT energies for the S_0 state are ~0.02 a.u. lower than the S_0 state energy calculated with full CI, but the energies for the S_2 state are an order of magnitude lower: by 0.14 a.u. for LSDA and 0.16 a.u. for PBE. The discrepancy between DFT and CI for HeH^+ is not as drastic. We observe the same trend as seen with the H_2 ground state energies, with DFT overstabilizing S_0 by ~0.02 a.u. But the overstabilizing of S_2 by DFT is only ~0.04–0.05 a.u., making the HeH^+ overall $S_0 \rightarrow S_2$ energy gap much more in line with the CI results.

The H_2 DFT exchange and correlation energies, along with HF exchange energy for comparison, as a function of population of the bonding orbital are shown in Fig. 3. The variation in the exchange energy as a function of population is much stronger than that of the correlation energy. When the bonding orbital is fully populated, the PBE exchange energy is quite close to the exact exchange energy predicted by HF, while LSDA underestimates the exchange energy. This underestimation of the exchange energy by LSDA is compensated by the overestimation of the correlation energy. As the electron density is driven into the antibonding orbital, leaving the bonding orbital empty, the exchange energy becomes more negative until the final portion of electron density is driven from the bonding orbital. For complete population of the antibonding orbital, the HF exact energy becomes less negative, while the DFT exchange energies remain constant (LSDA) or become even more negative (PBE). This disproportionate favoring of the doubly excited state leads to a much smaller energy gap. It is thus clear that while the adiabatic approximation of TDDFT can be used to excite the electronic density to the doubly excited state, the DFT energies of the excited state density may not be accurate.

TABLE II. The ground S_0 and doubly excited S_2 state dipoles (in a.u.) of minimal basis HeH^+. The two atoms of HeH^+ are equally spaced around the origin at ±0.4647 Å.

Method	S_0 μ	S_2 μ
HF	−0.53	2.81
LSDA	−0.45	2.84
PBE	−0.47	2.85
CI	−0.48	2.81

With the electron density of the doubly excited state, we can obtain not only the energies but also the molecular properties. The dipole moments of the S_0 and S_2 states for HeH^+ are shown in Table II. The HF/DFT dipoles of both states agree quite well with the CI results.

B. Linear response of the S_0 and S_2 states

To further elucidate the difference between single-reference linear response theory and the real-time nonperturbative method, we show how the solution of the linear response equation varies with changing molecular potential. Changes in the molecular potential in real-time TDHF/TDDFT are due to changes in the instantaneous electron distribution as a result of the time-dependent superposition of the S_0 and S_2 states. To set up the linear response matrices,[11,15] the orbital energies and related two-electron integrals are computed for both ψ_{S_0} and ψ_{S_2}. Figure 4 shows

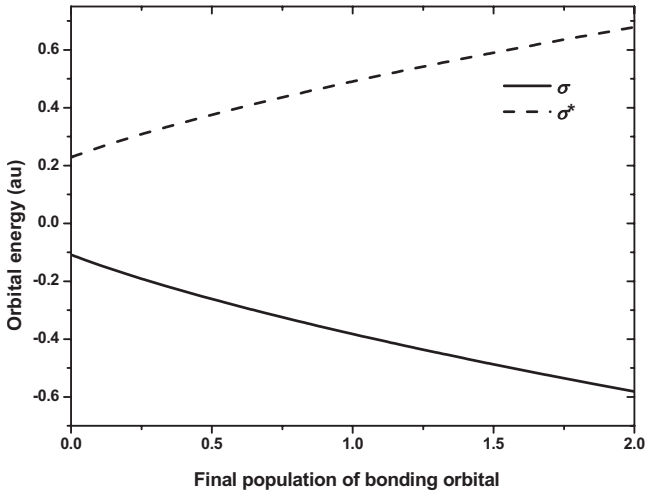

FIG. 4. H_2 real-time TDHF orbital energies as a function of excitation from the ground state.

that the H_2 real-time TDHF orbital energy gap decreases when electrons populate σ^*. When both electrons occupy the H_2 bonding σ_g orbital, the orbital energy difference is 1.26 a.u. When both electrons occupy the antibonding σ_u^* orbital, however, the orbital energy difference becomes −0.34 a.u. These values can be obtained from solving the standard time-independent HF equations for the orbital energies and are also observed in the real-time TDHF orbital energies, as given in Fig. 4. Table I gives the standard $S_0 \rightarrow S_1$ excitation energies from linear response TDHF, calculated with the ground state orbital energy gap and related two-electron integrals: $S_0 \rightarrow S_1$ $\Delta E = 0.94$ a.u. for H_2. If we calculate the H_2 linear response TDHF single-electron transition energy using the doubly excited S_2 state as the reference, the value obtained for de-exciting one electron from $S_2 \rightarrow S_1$ is $\Delta E = -0.61$ a.u.

In addition to choosing either the S_0 or S_2 state as a reference for solving the linear response equations, we can also choose a superposition state and solve the multireference linear response theory equations derived in the theory section. For H_2, when S_0 and S_2 each contribute 50% to the superposition state, the solution of Eq. (19) is 0.798 a.u., is in excellent agreement with the resonant field frequency $\omega = 0.80$ a.u., which leads to a full population inversion in real-time TDHF. Similar results are obtained for the solving for the superposition state of HeH^+. This clearly supports our rationale that the two-electron excitation resonance occurs at an energy that represents a solution of the multireference linear response function.

C. Dynamic absorption peak from the mixed potential of ground S_0 and doubly excited S_2 states

In real-time simulations, we can obtain transition information by monitoring the time-dependent dipole moment. The dipole continues to oscillate after the field is removed, indicating that the perturbation has induced mixing of other states into the reference state. The frequencies of oscillation are the energy gaps between states; Fourier transform of the residual dipole gives the absorption spectrum. CI predicts two peaks at the state energy gaps: $S_0 \rightarrow S_1$ and $S_1 \rightarrow S_2$. Because the dipole matrix element for transition between S_0 and S_2 is zero, the dipole oscillation is due to the mixing of the S_1 state with S_0 or S_2. The peaks vary in height according to the population of the S_0, S_1, and S_2 states. In contrast, Fourier transform of the real-time TDHF/TDDFT field-free time-dependent dipole affords a single peak in the absorption spectrum. The energy of this peak varies according to the ratio of population of the S_0 and S_2 states. Such behavior is consistent with predictions of the linear response of a superposition state, as shown in the previous section.

Figure 5 shows the energy of the TDHF absorption peak for H_2 and HeH^+ as a function of population of the bonding σ orbital. Near the ground state, the absorption peak energy corresponds to the $S_0 \rightarrow S_1$ linear response excitation energy calculated using the ground state potential (see Table I). As the population in σ decreases, the single peak in the Fourier transform shifts to lower energies for H_2 and to higher energies for HeH^+. The residual dipole oscillation frequency for

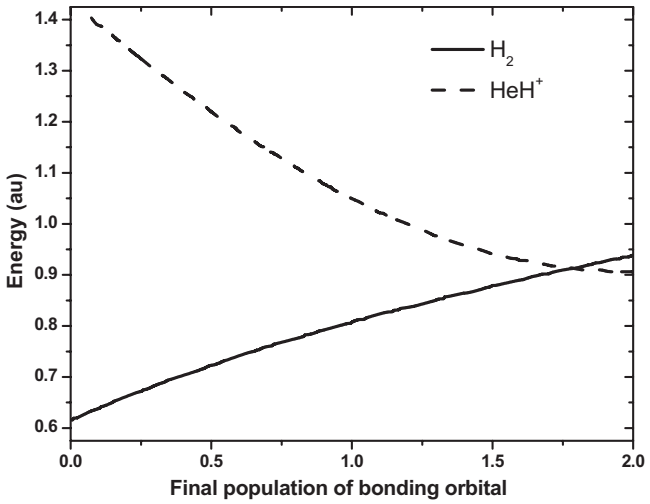

FIG. 5. Real-time TDHF absorption peak energy for H_2 and HeH^+ as a function of excitation from the ground state.

the S_2 state agrees with the linear response single-electron de-excitation energy, as discussed in the previous section. For H_2, the $S_2 \rightarrow S_1$ TDHF de-excitation energy is smaller than the $S_0 \rightarrow S_1$ excitation energy, so the peak shifts to lower energies. The opposite holds for HeH^+.

The shifting absorption peak reflects the same phenomena seen for the field-on electron optical response in Fig. 1. The behavior when the electrons are in the ground state agrees with the ground state linear response $S_0 \rightarrow S_1$ excitation energy. In Fig. 1, the greatest population change at low intensity is when the field frequency agrees with the linear response excitation energy of $\omega = 0.94$ a.u. for H_2 and $\omega = 0.90$ a.u. for HeH^+ (see Table I). As the system is excited, the potential changes, and both the field frequency ω, which shifts the most electron density, and the absorption peak shift. The energy of the absorption peak when both orbitals are equally occupied coincides with the resonant ω of the field that fully drives the electron density to oscillate between σ and σ^* and the solution of the linear response of a superposition state to which S_2 and S_0 each contribute 50%. Thus, within the single Slater determinant framework of TDHF/TDDFT, a dynamic absorption peak is the result of simultaneous single-electron processes: the $S_0 \rightarrow S_1$ excitation and the $S_2 \rightarrow S_1$ de-excitation.

IV. CONCLUSIONS

We have developed a real-time TDHF and adiabatic TDDFT approach that is beyond the perturbative regime. We have shown that adiabatic TDHF/TDDFT is able to simultaneously excite two electrons from the ground S_0 state to the doubly excited S_2 state and that the real-time TDHF/TDDFT implicitly includes double excitation within a superposition state. The two-electron potential is constantly updated with the instantaneous electron density within a closed-shell configurational space and thus behaves as an average potential of the S_0 and S_2 states. The electron density response in real-time TDHF/TDDFT corresponds to a superposition of perturbative linear responses of the S_0 and S_2 states, which agrees with our development of a frequency domain mut-

lireference linear response theory. We define the electron density of the S_2 state as the point when the dipole oscillation amplitude approaches zero. This occurs at a complete double occupation of σ^* for H_2 and at near double occupation of σ^* for HeH^+.

The TDHF/TDDFT residual dipole of two-electron, two-orbital H_2 and HeH^+ oscillates at a single frequency that shifts as the population is driven from S_0 to S_2. The Fourier transform of this residual dipole shows that the absorption peak shifts to lower energies for H_2 and higher energies for HeH^+ between solutions of the linear response of the S_0 and S_2 states. As supported by our TDHF frequency domain multireference linear response calculations, this shift in the absorption peak energy is due to the superposition of the $S_0 \rightarrow S_1$ single-electron excitation and the $S_2 \rightarrow S_1$ single-electron de-excitation. This result also explains the TDHF energy shift in the π-π^* transition of ethene observed by Eshuis *et al.*[29] The absorption peak energy at the point of equal population of S_0 and S_2 is the energy of resonant field frequency that fully drives the electron population between the S_0 and S_2 states.

With the doubly excited state electron density, we are able to calculate the properties of the S_2 state, such as the energy and dipole moment, with HF and DFT methods. Compared to the CI values, the $S_0 \rightarrow S_2$ energy gap is underestimated for both H_2 and HeH^+. This is a greater problem for DFT than HF because the S_2 DFT energy is calculated with an exchange-correlation functional that is designed to give energies for the ground state. The HeH^+ dipole moments are in good agreement with the CI dipoles for both the ground S_0 and doubly excited S_2 states.

ACKNOWLEDGMENTS

This research is supported by the National Science Foundation [Grant Nos. 0628252 (CHE-CRC) and 0835543 (PHY-CDI)] and by the ACS-Petroleum Research Fund (Grant No. 46487-G6). We would like to thank Berny Schlegel for insightful comments and the use of the CI MATHEMATICA notebook. Discussions with Oleg Prezhdo and Ernest Davidson are greatly appreciated. C.M.I. is supported by a UIF nanotechnology fellowship.

[1] M. Gavrila, *Atoms in Intense Laser Fields* (Academic, Boston, 1992).
[2] A. Zewail, J. Phys. Chem. A **104**, 5660 (2000).
[3] R. J. Cave and E. R. Davidson, J. Phys. Chem. **91**, 4481 (1987).
[4] B. E. Kohler, J. Chem. Phys. **88**, 2788 (1988).
[5] J. H. Starcke, M. Wormit, J. Schirmer, and A. Dreuw, Chem. Phys. **329**, 39 (2006).
[6] I. A. Mikhailov, S. Tafur, and A. E. Masunov, Phys. Rev. A **77**, 012510 (2008).
[7] A. Nozik, Inorg. Chem. **44**, 6893 (2005).
[8] V. I. Klimov, Annu. Rev. Phys. Chem. **58**, 635 (2007).
[9] C. M. Isborn, S. V. Kilina, X. Li, and O. V. Prezhdo, J. Phys. Chem. C **112**, 18291 (2008).
[10] K. C. Kulander, Phys. Rev. A **36**, 2726 (1987).
[11] A. Dreuw and M. Head-Gordon, Chem. Rev. (Washington, D.C.) **105**, 4009 (2005).
[12] E. Runge and E. K. U. Gross, Phys. Rev. Lett. **52**, 997 (1984).
[13] K. Yabana and G. F. Bertsch, Phys. Rev. B **54**, 4484 (1996).
[14] K. Burke, J. Werschnik, and E. K. U. Gross, J. Chem. Phys. **123**, 062206 (2005).
[15] R. E. Stratmann, G. E. Scuseria, and M. J. Frisch, J. Chem. Phys. **109**, 8218 (1998).
[16] M. E. Casida, in *Recent Advances in Density-Functional Methods*, edited by D. A. Chong (World Scientific, Singapore, 1995), pp. 155–193.
[17] M. E. Casida, in *Theoretical and Computational Chemistry*, edited by J. M. Seminario (Elsevier, Amsterdam, 1996), Vol. 4.
[18] D. B. Cook, *Oxford Science Publications* (Oxford University Press, Oxford, NY, 1998).
[19] R. Bauernschmitt and R. Ahlrichs, Chem. Phys. Lett. **256**, 454 (1996).
[20] D. Bohm and D. Pines, Phys. Rev. **92**, 609 (1953).
[21] H. Ehrenreich and M. H. Cohen, Phys. Rev. **115**, 786 (1959).
[22] M. Madjet, C. Guet, and W. R. Johnson, Phys. Rev. A **51**, 1327 (1995).
[23] X. Li, S. M. Smith, A. N. Markevitch, D. A. Romanov, R. J. Levis, and H. B. Schlegel, Phys. Chem. Chem. Phys. **7**, 233 (2005).
[24] F. Calvayrac, P. G. Reinhard, E. Suraud, and C. A. Ullrich, Phys. Rep. **337**, 493 (2000).
[25] G. F. Bertsch, J.-I. Iwata, A. Rubio, and K. Yabana, Phys. Rev. B **62**, 7998 (2000).
[26] A. Tsolakidis, D. Sánchez-Portal, and R. M. Martin, Phys. Rev. B **66**, 235416 (2002).
[27] Y. Takimoto, F. D. Vila, and J. J. Rehr, J. Chem. Phys. **127**, 154114 (2007).
[28] X. Andrade, S. Botti, M. A. L. Marques, and A. Rubio, J. Chem. Phys. **126**, 184106 (2007).
[29] H. Eshuis, G. G. Balint-Kurti, and F. R. Manby, J. Chem. Phys. **128**, 114113 (2008).
[30] S. Smith, X. Li, A. Markevitch, D. Romanov, R. Levis, and H. Schlegel, J. Phys. Chem. A **109**, 5176 (2005).
[31] S. Smith, X. Li, A. Markevitch, D. Romanov, R. Levis, and H. Schlegel, J. Phys. Chem. A **109**, 10527 (2005).
[32] S. Smith, X. Li, A. Markevitch, D. Romanov, R. Levis, and H. Schlegel, J. Phys. Chem. A **111**, 6920 (2007).
[33] S. Tretiak and V. Chernyak, J. Chem. Phys. **119**, 8809 (2003).
[34] P. Salek, O. Vahtras, T. Helgaker, and H. Agren, J. Chem. Phys. **117**, 9630 (2002).
[35] S. J. A. van Gisbergen, J. G. Snijders, and E. J. Baerends, J. Chem. Phys. **109**, 10644 (1998).
[36] S. J. A. van Gisbergen, J. G. Snijders, and E. J. Baerends, Phys. Rev. Lett. **78**, 3097 (1997).
[37] A. Masunov and S. Tretiak, J. Phys. Chem. B **108**, 899 (2004).
[38] P. N. Day, K. A. Nguyen, and R. Pachter, J. Chem. Phys. **125**, 094103 (2006).
[39] E. Badaeva and S. Tretiak, Chem. Phys. Lett. **450**, 322 (2008).
[40] N. T. Maitra, F. Zhang, R. J. Cave, and K. Burke, J. Chem. Phys. **120**, 5932 (2004).
[41] J. Neugebauer, E. J. Baerends, and M. Nooijen, J. Chem. Phys. **121**, 6155 (2004).
[42] C. A. Ullrich, J. Chem. Phys. **125**, 234108 (2006).
[43] B. G. Levine, C. Ko, J. Quenneville, and T. J. Martinez, Mol. Phys. **104**, 1039 (2006).
[44] M. E. Casida, J. Chem. Phys. **122**, 054111 (2005).
[45] R. J. Cave, F. Zhang, N. T. Maitra, and K. Burke, Chem. Phys. Lett. **389**, 39 (2004).
[46] H. B. Schlegel, S. M. Smith, and X. Li, J. Chem. Phys. **126**, 244110 (2007).
[47] C. M. Isborn, X. Li, and J. C. Tully, J. Chem. Phys. **126**, 134307 (2007).
[48] X. Li and J. C. Tully, Chem. Phys. Lett. **439**, 199 (2007).
[49] M. J. Frisch, G. W. Trucks, H. B. Schlegel *et al.*, GAUSSIAN DEVELOPMENT VERSION, Revision D.02, Gaussian, Inc., Wallingford, CT, 2004.
[50] W. Kohn and L. J. Sham, Phys. Rev. **140**, A1133 (1965).
[51] J. P. Perdew, K. Burke, and M. Ernzerhof, Phys. Rev. Lett. **77**, 3865 (1996).